Chiral Adsorption Structures of Styrene on Ge(001): A First-Principles Study

ARTICLE *in* THE JOURNAL OF PHYSICAL CHEMISTRY C · APRIL 2007

Impact Factor: 4.77 · DOI: 10.1021/jp066247l

2 AUTHORS, INCLUDING:

Hyung-Jin Kim
Dongguk University
22 PUBLICATIONS **116** CITATIONS

SEE PROFILE

Chiral Adsorption Structures of Styrene on Ge(001): A First-Principles Study

Hyung-Jin Kim and Jun-Hyung Cho*

BK21 Program Division of Advanced Research and Education in Physics, Hanyang University, 17 Haengdang-Dong, Seongdong-Ku, Seoul 133-791, Korea

Received: September 24, 2006; In Final Form: January 26, 2007

We investigated the chiral adsorption structures of styrene on the Ge(001) surface by first-principles density functional calculations within the generalized gradient approximation. Our calculated energy profile for the reaction pathways shows that styrene adsorbs not only on top of a single dimer but also across the ends of two adjacent dimers in the same dimer row. In the latter adsorption configuration (termed the "end-bridge" configuration), we predict the existence of two different structures where two unsaturated Ge atoms within the two adjacent dimers are differently displaced up and down or down and up. Additional styrene adsorption on these two different end-bridge structures proceeds to formation of the cis- and trans-paired end-bridge (PEB) structures. The relative stability of the two different end-bridge structures provides an explanation for a recent scanning tunneling microscopy observation that the populations of the *cis*-PEB and *trans*-PEB structures are different from each other.

Introduction

The chirality of organic molecules on surfaces has attracted much attention because of its role in stereoselective heterogeneous catalysis and chemical sensing.[1−13] Recently, chiral effects on surfaces such as a transfer[5] of chirality and a spontaneous separation[6] of enantiomers were reported. Since such an enantioselectivity is usually driven by the steric interaction between adsorbed molecules, the study of the atomic geometries of possible enantiomers on surfaces is an essential prerequisite for understanding the mechanisms of enantioselective surface chemistry. Most of previous studies of the enantioselective surface chemistry have concentrated on metal surfaces,[4,5,7−9] whereas relatively little work was spent on semiconductor surfaces.[10−13]

Using scanning tunneling microscopy (STM), Lopinski et al.[10] have determined the chirality of adsorbed propylene, *cis*-2-butene, and *trans*-2-butene on the Si(001) surface. Here, each prochiral molecule becomes a chiral species after adsorption on Si(001), producing a chiral adsorption system. Recently, the STM study of Hwang et al.[13] also observed several chiral structures of styrene when reacted with the Ge(001) surface. The observed chiral structures were classified into the two different adsorption configurations: One is the on-top (OT) configuration where one styrene adsorbs on top of a single dimer (see Figure 1a,b), and the other is the paired end-bridge (PEB) configuration where two styrenes adsorb across both ends of two adjacent dimers in the same dimer row (see Figure 1c−e). There are two kinds of OT structures: the (*R*) and (*S*) chiral structures. On the other hand, the PEB configuration has three different chiral structures according to the orientation of the phenyl ring of each styrene molecule: the diastereomeric (*R*,*S*) and the enantiomeric (*R*,*R*) and (*S*,*S*) chiral structures. It is notable that the average ratio of the (*R*,*S*), (*R*,*R*), and (*S*,*S*) populations was measured[13] as 1:1.4:1.4 at room temperature, showing that the dimeric adsorption of styrene on Ge(001) involves a relatively smaller population of the diastereomeric (*R*,*S*) structure compared to those of the enantiomeric (*R*,*R*) and (*S*,*S*) structures.

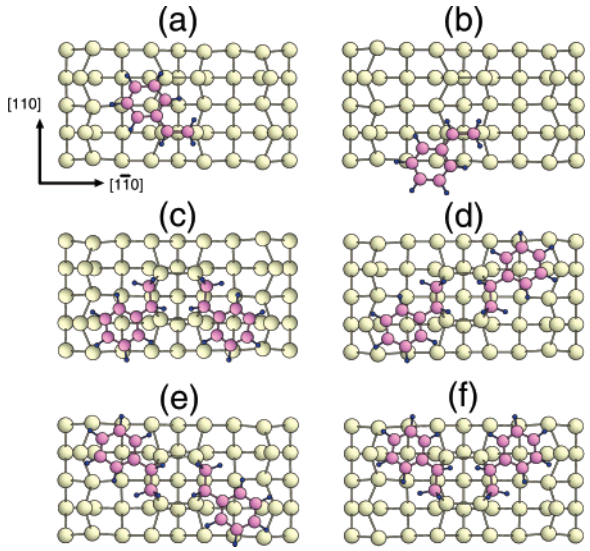

Figure 1. Top view of the optimized structure of adsorbed styrene on Ge(001): (a) the (*R*)-OT structure, (b) the (*S*)-OT structure, (c) the (*R*,*S*)-PEB structure, (d) the (*R*,*R*)-PEB structure, (e) the (*S*,*S*)-PEB structure, and (f) the (*S*,*R*)-PEB structure. The circles represent Ge, C, and H atoms with decreasing size.

In this paper, using first-principles density functional theory calculations, we investigated not only the binding energy and structure of adsorbed styrene on Ge(001), but also the reaction pathways for styrene adsorption. We found that the (*R*,*R*)- and (*S*,*S*)-PEB structures which have an identical adsorption energy (E_{ads}) of 0.99 eV are more stable than the (*R*,*S*)-PEB and OT structures by $\Delta E_{ads} = 0.24$ and 0.16 eV, respectively. Here, the PEB configuration can be formed after formation of the single end-bridge (SEB) configuration where one styrene adsorbs across the ends of two adjacent dimers in the same dimer row. Our calculated energy profile for the reaction pathways shows that formation of the OT and SEB structures takes place through

* chojh@hanyang.ac.kr.

10.1021/jp066247l CCC: $37.00
Published on Web 03/09/2007

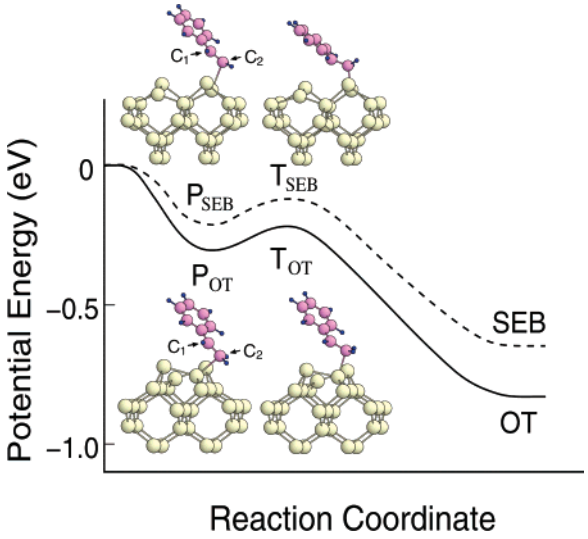

Figure 2. Calculated energy profiles for the reaction pathways forming the OT and SEB structures. The atomic geometries of the precursor and transition states along each reaction pathway are given.

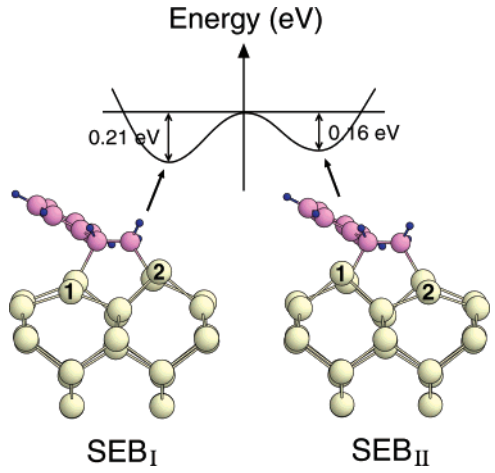

Figure 3. Energetics and geometries of the SEB_I and SEB_{II} structures. The energy barriers between the two structures are given.

their precursor states (see Figure 2), which are easily produced because of the energetically favored hybridization between the π bonding state of the C═C double bond of styrene and the empty dangling bond state of the down atom of the buckled Ge dimer. As shown in Figure 3, there are two kinds of SEB structures (designated as SEB_I and SEB_{II}) owing to the two possible up and down displacements of two unsaturated Ge atoms within the reacted two adjacent dimers. Since the dangling bond of the unsaturated down Ge atom in the SEB configuration can react with the π bond of another styrene, SEB_I and SEB_{II} will proceed to the formation of the (*R*,*R*)- [or (*S*,*S*)-] and (*R*,*S*)-PEB structures, respectively. On the basis of our calculated energetics, which shows that SEB_I is thermodynamically favored over SEB_{II}, we can say that the (*R*,*R*)- and (*S*,*S*)-PEB structures are likely to be more occupied as compared to the (*R*,*S*)-PEB structure, consistent with the STM data of Hwang et al.[13]

Calculation Method

The total energy and force calculations were performed by using first-principles density functional theory within the generalized-gradient approximation (GGA).[14,15] We used the exchange-correlation functional of Perdew et al.[15] for the GGA. The norm-conserving pseudopotentials of Ge and H atoms were constructed by the scheme of Troullier and Martins[16] in the separable form of Kleinman and Bylander.[17] For the C atom whose 2s and 2p valence orbitals are strongly localized, we used the Vanderbilt ultrasoft pseudopotentials.[18] The surface was modeled by periodic slab geometry. Each slab contained six Ge atomic layers, and the bottom Ge layer was passivated by two H atoms per Ge atom. The thickness of the vacuum region between these slabs is about 15 Å, and styrene molecules were adsorbed on the unpassivated side of the slab. A plane-wave basis set was used with a 25 Ry cutoff, and the **k** space integration was done with meshes of 2 **k** points in the 4 × 2 surface Brillouin zone. All the atoms except the bottom two Ge layers were allowed to relax along the calculated Hellmann−Feynman forces until all the residual force components were less than 1 mRy/bohr.

TABLE 1: Calculated Adsorption Energies (in eV) per Styrene Molecule for Various Precursor (P), Transition (T), and Chemisorption (C) States

	P	T	C	E_b[a]
OT	0.30	0.23	0.83	0.07
SEB	0.21	0.12	0.65	0.09
(*R*,*R*)-PEB	0.23[b]	0.14[b]	0.99	0.09
(*R*,*S*)-PEB	0.22[b]	0.09[b]	0.75	0.13

[a] E_b denotes the energy barrier from the P to the C states. [b] The adsorption energies for the precursor and transition states along the reaction pathway forming the (*R*,*S*)- and (*R*,*R*)-PEB structures are calculated as the difference in the total energy of an additional styrene on the corresponding SEB structure from its separated limit (i.e., a free styrene plus SEB): see text.

Results

First, we optimized the atomic structure of adsorbed styrene on Ge(001) within the OT and PEB configurations. Here, we used a 4 × 2 unit cell which involves four Ge dimers within two dimer rows. The styrene molecule belongs to the alkene group, containing a double C═C bond. It is well-known that the adsorption of alkenes on Si(001) takes place through the so-called [2 + 2] cycloaddition reaction,[19,20] where the π bond of alkenes interacts with the π bonds of the Si dimers, forming two new Si−C σ bonds. Note that the OT and PEB configurations for adsorbed styrene on Ge(001) are the [2 + 2] products on top of a single dimer and across both ends of two adjacent dimers, respectively. The optimized structures for the OT and PEB configurations are shown in Figure 1, and their calculated adsorption energies are given in Table 1. As shown in Figure 1a,b, there are two possible (*R*) and (*S*) chiral products in the OT configuration. Here, the (*R*) and (*S*) structures, which are mirror-symmetric to each other with a (110) plane containing the reacted Ge dimer, are determined by the attack direction of styrene to the Ge dimer. On the other hand, the PEB configuration has three kinds of chiral products according to the orientation of the phenyl ring of each styrene molecule: the diastereomeric (*R*,*S*) and the enantiomeric (*R*,*R*) and (*S*,*S*) structures (see Figure 1c−e, respectively). We find that the (*R*,*R*)- and (*S*,*S*)-PEB structures, which have an identical adsorption energy of 0.99 eV, are more stable than the (*R*,*S*)-PEB structure by $\Delta E_{ads} = 0.24$ eV (here, the adsorption energies of the PEB structures are given per molecule). This enhanced adsorption energy of the former two PEB structures may be due to a relatively greater reduction in the repulsive H−H interaction between the phenyl rings of the two adsorbed styrene molecules, compared to the case of the latter PEB structure. However, it should be cautioned that the DFT calculations cannot appropriately account for dispersion interactions and often overpredict the degree of repulsion. We also find that the

(*R*,*R*)- and (*S*,*S*)-PEB structures are more stable than the (*R*)- and (*S*)-OT structures by $\Delta E_{ads} = 0.16$ eV (see Table 1).

Recent experimental[19,20] and theoretical[21] studies reported that the reaction of alkenes on Si(001) occurs via a precursor in which the electrophilic down atom (positively charged) of the buckled Si dimer attracts the π electrons of the C═C bond. Note that there are two models for the precursor state before formation of the [2 + 2] product. One is the "three-atom" model, which is composed of a three-membered ring with the down Si atom and the two C atoms.[20,21] The other is the "diradical" model where the π bond of C═C is broken to create a single Si—C bond and a radical.[22] For examples, the precursor state in adsorbed ethylene (having a nonpolar C═C bond) on Si(001) belongs to the three-atom model,[21] while that in adsorbed vinyl bromide (having a polar C═C bond) on Si(001) belongs to the diradical model.[22] Considering that the C═C bond of styrene is partly polarized because of a greater electronegativity of the phenyl ring compared to the H atoms attached to the C═C bond, we expect that the C atom bonded to two H atoms would be more attracted to the electrophilic down Ge atom compared to the C atom bonded to the phenyl ring and one H atom. Therefore, the precursor state in adsorbed styrene on Ge(001) might belong to the diradical model. In the present study, we assume that formation of the precursor state takes place without an energy barrier. The optimized structures for the precursor states (designated as P_{OT} and P_{SEB}, respectively) along the reaction pathways forming the OT and SEB configurations are displayed in Figure 2. Here, the direction of the C═C bond in P_{OT} (P_{SEB}) is parallel (perpendicular) to the Ge dimer bond. In the P_{OT} (P_{SEB}) state, the calculated distance $d_1 = 2.76(3.19)$ Å between the C_1 atom and the down Ge atom is much longer than $d_2 = 2.42(2.54)$ Å between the C_2 atom and the down Ge atom (see Figure 2). This result indicates that the C_2 atom bonded to two H atoms is more easily attracted to the positively charged down Ge atom as compared to the C_1 atom bonded to the phenyl ring and one H atom. Thus, as expected, the P_{OT} and P_{SEB} states belong to the diradical model. The calculated adsorption energies of P_{OT} and P_{SEB} are given in Table 1. We find that P_{OT} has an adsorption energy of 0.30 eV, slightly larger than that (E_{ads}= 0.21 eV) of P_{SEB}.

Next, we calculated the energy profile along the reaction pathway from the precursor to the chemisorption states. In order to find the minimum energy pathway, we optimized the structure by using the gradient projection method[23] where only the distance d_{C1-Ge} (but not angles) between the C_1 atom and its bonded (in the chemisorption state) Ge atom was constrained. Therefore, we obtain the energy profile for the reaction pathway as a function of decreasing distance d_{C1-Ge}. Here, Hellmann—Feynman forces aid in the relaxation of all the atomic positions as well as the C_1—Ge bond angles for each fixed value of d_{C1-Ge}. The calculated energy profiles and atomic geometries of the transition states (designated as T_{OT} and T_{SEB}, respectively) along the reaction pathways forming the OT and SEB configurations are displayed in Figure 2. We find that the T_{OT} (T_{SEB}) state has $E_{ads} = 0.23$ (0.12) eV, which is 0.07 (0.09) eV smaller than that of the P_{OT} (P_{SEB}) state, thereby yielding an energy barrier $E_b = 0.07$ (0.09) eV from the P_{OT} (P_{SEB}) state to the OT (SEB) configuration. We also find that the barrier for the rotation of the precursor state (from P_{SEB} to P_{OT}) amounts to ~0.1 eV, comparable with $E_b = 0.09$ eV from P_{SEB} to SEB. This result implies that either the rotation from P_{SEB} to P_{OT} or the transition from P_{SEB} to SEB is equally probable. However, both because the SEB configuration can bond in either of two directions, while the OT configuration can only bond in one, and also because the values of E_b for formation of the OT and SEB configurations are similar to each other, we expect that the OT and SEB configurations would be almost equally occupied via the P_{OT} and P_{SEB} states.

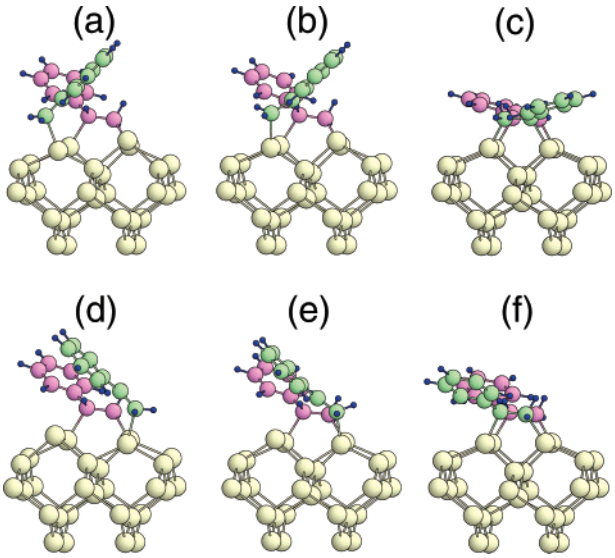

Figure 4. Atomic geometries of the precursor (P), transition (T), and chemisorption states along the reaction pathways forming the (*R*,*R*)- and (*R*,*S*)-PEB structures: (a) the P_{RR-PEB} structure, (b) the T_{RR-PEB} structure, (c) the (*R*,*R*)-PEB structure, (d) the P_{RS-PEB} structure, (e) the T_{RS-PEB} structure, and (f) the (*R*,*S*)-PEB structure.

In the SEB configuration, a styrene breaks π bonds on each of the two Ge dimers to which it is bonded, leaving highly reactive π-electrons on the dimer atoms (i.e., Ge_1 and Ge_2 in Figure 3) to which it is not bonded. It is noticeable that there are two kinds of SEB structures (see Figure 3, labeled SEB_I and SEB_{II}) depending on the different vertical displacements of Ge_1 and Ge_2. In SEB_I (SEB_{II}), the Ge_1 and Ge_2 atoms are displaced down and up (up and down), respectively. We find that SEB_I which has $E_{ads} = 0.65$ eV is more stable than SEB_{II} by ΔE_{ads}= 0.05 eV. We also find that the energy barrier from SEB_I (SEB_{II}) to SEB_{II} (SEB_I) is 0.21 (0.16) eV.[24] Using an Arrhenius-type activation process with a typical vibration frequency (~10^{13} Hz) for the preexponetial factor, we estimate that at room temperature the converting rate from SEB_I (SEB_{II}) to SEB_{II} (SEB_I) is ~3.0×10^9 (2.0×10^{10}) s^{-1}, indicating a rapid vertical motion of Ge_1 and Ge_2 between SEB_I and SEB_{II}. Thus, from the calculated energetics (ΔE_{ads}= 0.05 eV) between SEB_I and SEB_{II}, at room temperature, SEB_I is ~7 times more likely to be occupied at any time than SEB_{II}.

The remaining highly reactive π-electrons in the SEB_I and SEB_{II} structures can react with the C═C bond of another styrene molecule, forming the PEB configuration. Noting that the electrophilic down Ge atom attracts the π bond of styrene, SEB_I (SEB_{II}) in which Ge_1 (Ge_2) is the down atom leads to formation of the (*R*,*R*)-PEB ((*R*,*S*)-PEB) structure. Along the reaction pathway forming the (*R*,*R*)-PEB structure, the precursor (P_{RR-PEB}; see Figure 4a) and transition (T_{RR-PEB}; see Figure 4b) states of an additional styrene on SEB_I are stabilized over its separated limit (i.e., a free styrene plus SEB_I) by $\Delta E = 0.23$ and 0.14 eV, respectively. Therefore, we obtain $E_b = 0.09$ eV from the P_{RR-PEB} state to the (*R*,*R*)-PEB structure. On the other hand, along the reaction pathway from SEB_{II} to (*R*,*S*)-PEB, we find that the precursor state (P_{RS-PEB}; see Figure 4d) of an additional styrene on SEB_{II} is stabilized over its separated limit (i.e., a free styrene plus SEB_{II}) by $\Delta E = 0.22$ eV and that this P_{RS-PEB} state proceeds to the formation of (*R*,*S*)-PEB through the

transition (T_{RS-PEB}; see Figure 4e) state with $E_b = 0.13$ eV. On the basis of our calculated energy profiles for the two reaction pathways, we can say that the formation of the (*R*,*R*)- and (*R*,*S*)-PEB structures can be facilitated at room temperature because of the existence of their low activation barriers.

A recent room-temperature STM study of Hwang et al.[13] measured the populations of three different chiral PEB structures for adsorbed styrene on Ge(001). The average ratio of the *cis*-PEB, (*R*,*R*)-*trans*-PEB, and (*S*,*S*)-*trans*-PEB populations was 1:1.4:1.4. As pointed out by Hwang et al.,[13] this result may reflect that the *trans*-PEB structures are more stable than the *cis*-PEB structure, consistent with our calculated energetics for those structures (see Table 1). However, it is more likely that the different populations of the *trans*-PEB and *cis*-PEB structures would be determined by the energetics of their precedent structures (i.e., SEB_I and SEB_{II}, respectively). Our estimation that the SEB_I population is ~7 times larger than the SEB_{II} population at room temperature qualitatively accounts for the observed[13] greater population of *trans*-PEB as compared to that of *cis*-PEB. Since both (*R*,*S*)-PEB and (*S*,*R*)-PEB (see Figure 1f) are treated as an identical *cis*-PEB structure, the actual ratio of the (*R*,*S*)-PEB and (*R*,*R*)-PEB populations should be 0.5:1.4 = 1:2.8. However, this ratio is still less than our estimated ratio (1:6.9) of the SEB_{II} and SEB_I populations. This quantitative difference between experiment[13] and our estimation may be due to a somewhat overestimation of our calculated energy difference between SEB_I and SEB_{II}, caused by the use of a rather small 4×2 unit cell.

Summary

We have performed first-principles density functional calculations for the adsorption of styrene on the Ge(001) surface. Our calculated energy profiles for the reaction pathways support recent[13] STM data for formation of the OT and PEB structures. Especially, we found the existence of two different SEB structures where the two unsaturated Ge atoms are differently displaced up and down or down and up. These two SEB structures proceed to formation of the *cis*- and *trans*-PEB structures. Thus, we conclude that the relative stability of the two SEB structures possibly determines a different population ratio between the *trans*-PEB and *cis*-PEB structures, as observed by the recent STM experiment of Hwang et al.[13]

Acknowledgment. This work was supported by grants from the Basic Research Program (no. R01-2006-000-10920-0) of the Korea Science & Engineering Foundation, by the Korea Research Foundation Grant funded by the Korean Government (MOEHRD) (KRF-2005-003-C00053), and by the MOST/KOSEF through the Quantum Photonic Science Research Center.

References and Notes

(1) Rowan, A. E.; Nolte, R. J. M. *Angew. Chem., Int. Ed.* **1998**, *37*, 63, and references therein.

(2) McKendry, R.; Theoclitou, M.-E.; Rayment, T.; Abell, C. *Nature (London)* **1998**, *391*, 566.

(3) Carmeli, I.; Skakalova, V.; Naaman, R.; Vager, Z. *Angew. Chem., Int. Ed.* **2002**, *41*, 761.

(4) Farsel, R.; Wider, J.; Quitmann, C.; Ernst, K.-H.; Greber, T. *Angew. Chem., Int. Ed.* **2004**, *43*, 2853.

(5) Farsel, R.; Parschau, M.; Ernst, K.-H. *Angew. Chem., Int. Ed.* **2003**, *42*, 5178.

(6) Weisbuch, I.; Kuzmenko, I.; Berfeld, M.; Leiserowitz, L.; Lahav, M. *J. Phys. Org. Chem.* **2000**, *13*, 426.

(7) Ohtani, B.; Shintani, A.; Uosaki, K. *J. Am. Chem. Soc.* **1999**, *121*, 6515.

(8) Lorenzo, M.; Baddeley, C. J.; Muryn, C.; Raval, R. *Nature (London)* **2000**, *404*, 376.

(9) Kühnle, A.; Linderoth, T. R.; Hammer. B; Besenbacher. F. *Nature (London)* **2002**, *415*, 891.

(10) Lopinski, G. P.; Moffatt, D. J.; Wayner, D. D. M.; Wolkow, R. A. *Nature (London)* **1998**, *392*, 909.

(11) Lopinski, G. P.; Moffatt, D. J.; Wayner, D. D. M.; Wolkow, R. A. *J. Am. Chem. Soc.* **2000**, *122*, 3548.

(12) Kim, J. W.; Carbone, M.; Dil, J. H.; Tallarida, M.; Flammini, R.; Casaletto, M. P.; Horn, K.; Piancastelli, M. N. *Phys. Rev. Lett.* **2005**, *95*, 107601.

(13) Hwang, Y. J.; Kim, A. S.; Hwang, E. K.; Kim, S. H. *J. Am. Chem. Soc.* **2005**, *127*, 5016.

(14) Hohenberg, P.; Kohn, W. *Phys. Rev.* **1964**, *136*, B864. Kohn, W.; Sham, L. J. *Phys. Rev.* **1965**, *140*, A1133.

(15) Perdew, J. P.; Burke, K.; Ernzerhof, M. *Phys. Rev. Lett.* **1996**, *77*, 3865.

(16) Troullier, N.; Martins, J. L. *Phys. Rev. B* **1991**, *43*, 1993.

(17) Kleinman, L. D.; Bylander, M. *Phys. Rev. Lett.* **1982**, *48*, 1425.

(18) Vanderbilt, D. *Phys. Rev. B* **1990**, *41*, R7892. Laasonen, K.; Pasquarello, A.; Car, R.; Lee, C.; Vanderbilt, D. *Phys. Rev. B* **1993**, *47*, 10142.

(19) Liu, H.; Hamers, R. J. *J. Am. Chem. Soc.* **1997**, *119*, 7593.

(20) Nagao, M.; Mukai, K.; Yamashita, Y.; Yoshinobu, J. *J. Phys. Chem. B* **2004**, *108*, 5703.

(21) Cho, J.-H.; Kleinman, L. *Phys. Rev. B* **2004**, *69*, 075303.

(22) Cho, J.-H.; Kleinman, L. *Phys. Rev. B* **2005**, *71*, 125330.

(23) Wismer, D. A.; Chattery, R. *Introduction to Nonlinear Optimization*; North-Holland: Amsterdam, 1978; pp 174−178.

(24) We obtained the transition state between SEB_I and SEB_{II} by optimizing the structure in which both the Ge_1 and Ge_2 atoms have an identical height normal to the surface.